HHS Public Access

Author manuscript

Traffic. Author manuscript; available in PMC 2017 March 01.

Published in final edited form as:

Traffic. 2016 March ; 17(3): 230–244. doi:10.1111/tra.12354.

The Na+-Taurocholate Cotransporting Polypeptide Traffics with the Epidermal Growth Factor Receptor

Xintao Wang[1], **Pijun Wang**[1], **Wenjun Wang**[1,3], **John W. Murray**[1,3], and **Allan W. Wolkoff**[1,2,3]

[1]Marion Bessin Liver Research Center, Albert Einstein College of Medicine and Montefiore Medical Center, Bronx, NY 10461

[2]Division of Gastroenterology and Liver Diseases, Albert Einstein College of Medicine and Montefiore Medical Center, Bronx, NY 10461

[3]Department of Anatomy and Structural Biology, Albert Einstein College of Medicine and Montefiore Medical Center, Bronx, NY 10461

Abstract

Na^+-taurocholate cotransporting polypeptide (ntcp) mediates uptake of bile acids as well as serving as the receptor for hepatitis B virus in human liver. Previous studies showed that ntcp traffics on microtubules between the cell surface and endocytic vesicles. Specific inhibition of protein kinase C (PKC)ζ resulted in loss of microtubule-based motility of these vesicles in vitro and in living cells. The aim of the present study was to characterize the PKCζ target. Incubation of ntcp-containing endocytic vesicles with γ-^{32}P-ATP revealed a 180 kDa phosphoglycoprotein that was identified as the EGF receptor (EGFR). Surface biotinylation of HuH7 cells expressing GFP-ntcp revealed substantially reduced trafficking of ntcp to the cell surface with EGFR knockdown. Microtubule-based motility of ntcp-containing endocytic vesicles was also significantly reduced when they were not associated with EGFR. Ntcp was also found to undergo cellular redistribution upon stimulation of cells with EGF, consistent with a model in which ntcp and EGF-EGFR internalize into common endocytic vesicles from which they segregate, trafficking EGF-EGFR to lysosomes and recycling ntcp to the plasma membrane. EGF regulation of ntcp trafficking may play a heretofore unanticipated role in subcellular targeting of ntcp ligands such as hepatitis B.

Keywords

bile acid; drug transport; endosome; Hepatitis B virus (HBV); microtubule

Introduction

The Na^+-taurocholate cotransporting protein (ntcp) mediates Na^+-dependent uptake of bile acids as well as other organic anions (1). Recent studies have shown that it also serves as the

Address all correspondence to: Allan W. Wolkoff, Marion Bessin Liver Research Center and Division of Gastroenterology and Liver Diseases, Albert Einstein College of Medicine and Montefiore Medical Center, 517 Ullmann Building, 1300 Morris Park Ave, Bronx, NY 10461, USA, Tel.: (718) 430-3798, Fax: (718) 430-8568, allan.wolkoff@einstein.yu.edu.

Conflict of Interests

The authors have no conflict of interests to declare.

receptor for the hepatitis B virus in human hepatocytes (2–8). Previous studies revealed that ntcp can traffic between the cell surface and an intracellular vesicular pool (9,10). This subcellular trafficking requires intact microfilament- and microtubule-based cytoskeletons (10,11) and is regulated by activity of the PI3 kinase/PKCζ pathway (12–14). In further studies, a cell free system was developed in which ntcp-containing vesicles were found to bind to and move along microtubules (10,15–17). In these studies, microtubule-based motility of ntcp-containing vesicles was quantified in a fluorescent microtubule coated microassay chamber (10,18). Microtubule-bound vesicles that were labeled with antibody to ntcp followed by fluorescent secondary antibody moved bidirectionally on the microtubules following addition of ATP (10,18). These ntcp-containing vesicles colocalized with markers for recycling and early endocytic vesicles, but not with markers for late endocytic vesicles (10). Motility was attributed to association of these vesicles with the minus-end directed microtubule motor dynein, and with the plus-end directed microtubule motor kinesin-1 (10). These studies also showed that the transferrin receptor (TfR) traffics with ntcp and that they are colocalized in these vesicles (10,18). PKCζ was also found to be associated with these vesicles, and inhibition of PKCζ activity resulted in their loss of motility while motility of late endocytic vesicles remained unaffected (10). The target of PKCζ-mediated phosphorylation that regulates the motility of ntcp-containing endocytic vesicles is not known and its identification was the subject of the present study. In addition, the association of PKCζ with ntcp and TfR containing vesicles suggested the possibility that it plays a role in their internalization, and this was also examined.

Results

EGFR is Phosphorylated by PKCζ in ntcp-immunopurified vesicles

Rat liver derived endocytic vesicles incubated with γ-^{32}P-ATP in the presence or absence of PKCζ pseudosubstrate inhibitor, were subjected to SDS-PAGE and radioautography. Although several phosphorylated bands were observed when total endocytic vesicles were assayed (Figure 1A, left panel), none were sensitive to PKCζ inhibition. In contrast, in ntcp-immunopurified vesicles, a 180 kDa phosphoprotein sensitive to PKCζ inhibition was observed. This protein was a glycoprotein, as seen by its binding to Con A and WGA (Figure 1B) and sensitivity to PNGase F incubation (Figure 1C). Mass spectroscopic analysis of proteins in this region of the gel identified EGFR and clathrin as the major constituents (data not shown). However, following PNGase F incubation of phosphorylated immunopurified vesicles, there was a downward shift of radioactivity and EGFR on SDS-PAGE while mobility of clathrin remained unchanged (Figure 1D), suggesting that EGFR could be the phosphorylated target of PKCζ in these vesicles.

Preparation of an HuH7-derived cell line in which EGFR is knocked down

Human hepatoma-derived HuH7 cells stably expressing ntcp-sfGFP were infected with lentiviral particles encoding EGFR shRNA (EGFR KD) or empty plasmid (control). A representative Western blot, performed in duplicate, of lysates of these cells is shown in Figure 2A. Western blots of four independent studies were performed and densitometric quantification, normalized for actin expression, shows that EGFR expression was reduced

by approximately 80% while expression of ntcp was essentially unchanged in the EGFR KD as compared to control cells (Figure 2B).

Effect of EGFR colocalization on microtubule-based motility of ntcp-containing vesicles

Endocytic vesicles were prepared from control and EGFR KD ntcp-sfGFP expressing HuH7 cells, and colocalization of ntcp with EGFR was determined in a microscopy chamber. In 4 experiments, 33.1% ± 7.2% (mean ± SEM) of 328 ntcp-containing vesicles from control cells colocalized with EGFR, while only 6.1% ± 1.9% of 435 vesicles from EGFR KD cells colocalized with EGFR ($p<0.01$). A representative experiment is seen in Figure 3A. To examine the influence of EGFR colocalization on motility, vesicles were bound to microtubules in a microscopy chamber. Following ATP addition, over 20% of ntcp-containing vesicles from control cells moved as compared to 11% of ntcp-containing vesicles from EGFR KD cells (Figure 3B, $p<0.03$). Motility of ntcp-containing vesicles from control cells was sensitive to inhibition of PKCζ, falling by approximately 60% ($p<0.01$) (Figure 3B). In contrast, there was no effect of PKCζ inhibition on motility of ntcp-containing vesicles prepared from EGFR KD cells (Figure 3B). Additional studies were performed on vesicles isolated from parental ntcp-sfGFP expressing HuH7 cells that had not been infected with lentivirus. As seen in Figure 3C, these preparations included vesicles in which ntcp and EGFR are colocalized and vesicles that express ntcp in the absence of EGFR. Upon ATP addition, those vesicles containing both ntcp and EGFR had much greater motility; many fewer ntcp-containing vesicles that lacked EGFR moved along microtubules in the presence of ATP as compared to those that contained EGFR (Figures 3C and 3D, $p<0.01$).

Effect of EGFR colocalization on subcellular distribution and function of ntcp

Cell surface content of EGFR and ntcp were determined following surface biotinylation, pull down of biotinylated proteins on streptavidin-agarose, and analysis by Western blot. As seen in the representative study in Figure 4A, actin, an abundant intracellular protein, was not detected in the pull down (surface lanes), indicating that intracellular proteins were not labeled in these studies. As seen in Figure 4B, in 4 independent studies, after correction for volumes applied to the gel, approximately 50% of total EGFR was found on the cell surface in both control and EGFR knockdown cells, while the total EGFR content in knockdown cells was reduced by approximately 80% (Figures 2 and 4A). Cell surface expression of ntcp was also approximately 50% of total in control cells, but was reduced to approximately 30% of total in EGFR KD cells (Figure 4B). To see if this reduction of cell surface ntcp had an effect on bile acid transport, uptake of ^{3}H-taurocholic acid was quantified in lentiviral vector only infected control cells and EGFR KD cells. As seen in the representative study in Figure 4C and results of three studies presented in Table 1, there was no significant difference in the fitted parameters K_m, V_{max}, or k between control and EGFR knockdown cells ($p > 0.5$). Additional studies showed that uptake of 1 μM ^{3}H-taurocholic acid by ntcp-sfGFP expressing control and EGFR KD cells is highly Na^+-dependent (Figure 4D), as would be expected for ntcp-mediated transport that is well known to be Na^+-dependent (19).

Effect of EGF incubation on subcellular distribution of EGFR and ntcp in HuH7 cells stably expressing ntcp-sfGFP

The preceding studies indicate that ntcp and EGFR colocalize in a common intracellular compartment and that reduced cell content of EGFR is associated with reduced cell surface expression of ntcp while total cell content of ntcp is unchanged (Figure 4). To further characterize the relationship between ntcp and EGFR, studies were performed to examine their subcellular trafficking in intact HuH7 cells stably expressing ntcp-sfGFP. In addition, trafficking of the transferrin receptor (TfR) was also examined as our previous studies showed that the transferrin receptor (TfR) traffics with ntcp in PKCζ-associated vesicles (10,18). In these studies, cell surface proteins were biotinylated at 4°C with sulfo-NHS-biotin and then warmed to 37°C in the presence of EGF with and without PKCζ inhibition (PS) to permit internalization of biotinylated proteins. Biotin remaining on the cell surface was removed by reduction, and the recovered biotinylated internalized protein was analyzed by Western blot. These studies showed that surface EGFR, ntcp, and TfR internalize over time and this process is blocked by inhibition of PKCζ activity as seen in the representative study in Figure 5A. Quantitation of 3 independent studies showed that 10 min after incubation with EGF, approximately 20% of both EGFR (Figure 5B) and ntcp (Figure 5C) were internalized from the cell surface with little internalization of either protein when PKCζ activity was inhibited. Similar results were found for TfR, for which the fraction that was internalized was over 90% and was substantially reduced following inhibition of PKCζ activity (Figure 5D). These studies are consistent with the view that ntcp, TfR, and EGFR are internalized into a common endocytic vesicle and that this process requires PKCζ activity.

EGFR and ntcp follow different endocytic routes following internalization

It is known that EGF-EGFR complexes are internalized and traffic to lysosomes where they are degraded, while internalized TfR recycles to the cell surface and does not traffic to lysosomes (20). To determine the route followed by internalized ntcp, total cell content of EGFR and ntcp were quantified by Western blot following EGF incubation of HuH7 cells expressing ntcp-sfGFP with or without PKCζ inhibition. As seen in Figure 6, 60 min after incubation of cells with EGF, approximately 50% of EGFR was lost as the EGFR-EGF complex trafficked to lysosomes where it was degraded (21). However, degradation of EGFR was not seen when PKCζ activity was inhibited. In contrast, there was no significant change in cellular content of ntcp with or without PKCζ inhibition. These studies are consistent with a model in which ntcp and EGFR internalize into a common vesicle in the presence of EGF. However, the fact that EGFR, but not ntcp, is degraded suggests that these two proteins segregate from each other within the cell and target to different subcellular destinations. This is similar to our previous findings that vesicles containing ntcp and TfR segregate from asialoorosomucoid (ASOR), a ligand for the asialoglycoprotein receptor (ASGPR), that is present in these early vesicles but later traffics to lysosomes (18).

PKCζ activity is required for EGF mediated internalization of ntcp in HuH7 cells stably expressing ntcp-sfGFP

Internalization of ntcp was examined in HuH7 cells stably expressing ntcp-sfGFP by fluorescence microscopy (Figure 7). Incubation with EGF, resulted in dramatic redistribution of ntcp into ruffle-like structures, as exemplified in Figure 7A. Almost immediately after EGF incubation, ruffles containing ntcp began to form near the cell periphery as highlighted by drawn yellow lines at 4 min. The ruffles then progressed toward the cell center, being absorbed back into the cell 8–15 min after formation, with individual cell difference in the extent and progression of the ruffles. Previous findings have characterized such structures as EGF-stimulated dorsal ruffles that can selectively sequester and internalize activated EGFR away from other surface receptors (21). Figure 7A demonstrates that these dorsal ruffles can contain the bile acid transporter, ntcp. Interestingly, this redistribution of ntcp into ruffles was prevented by incubation of the cells with PKCζ pseudosubstrate inhibitor (PS) (Figure 7B), supporting the findings of Figure 5 that ntcp internalization is blocked in the presence of the inhibitor. Higher magnification imaging revealed that, as ruffles progressed to the cell center and reabsorbed into the cell (22,23), small ntcp containing extensions formed elsewhere as highlighted in yellow (Figure 7C). That ntcp redistribution into ruffles is not a generalized effect of receptor tyrosine kinase activity is seen in Figure 7D in which, as compared to results with EGF, there was little ruffling seen with insulin addition and none following PDGF addition to cells. This behavior suggests that, following EGF stimulation and endocytosis, ntcp can internalize at sites of ruffle reabsorption following which it redistributes into vesicles that traffic through the cell. This was seen in ntcp-sfGFP cells that were incubated with Alexa Fluor 555 labeled fluorescent EGF (Fl-EGF) and studied by live cell imaging. Similar to studies with unlabeled EGF, addition of Fl-EGF resulted in ruffle formation . Additionally the sites of ruffle reabsorption correspond with sites of Fl-EGF endosomal coalescence, as has been previously reported (22) as well as colocalization of Fl-EGF with ntcp (examples in Figure 8A,B, yellow lines highlighting colocalization). Over the ensuing minutes, EGF and ntcp exhibited decreased colocalization as they segregated from each other (Figure 8A, B).

Discussion

Ntcp is a hepatocyte specific 7 transmembrane domain protein that mediates uptake of bile acids from the circulation (1,24). Although it is localized to the basolateral (sinusoidal) plasma membrane of hepatocytes, it has been found to cycle between an intracellular vesicular pool and the plasma membrane (9,10,25,26). This process requires an intact cytoskeleton (11) and function of the PI3K/PKB pathway (12–14) to activate PKCζ, an atypical member of the PKC family (27,28). Recent studies in a cell free system that examined microtubule-based motility of ntcp-containing endocytic vesicles revealed bidirectional movement mediated by the plus-end motor kinesin-1 and the minus-end motor dynein (10,18). PKCζ colocalized to these vesicles and its activity was required for their motility (10,18). In the present study, we examined whether PKCζ activity was required for ntcp internalization. In addition, the vesicle-associated target of PKCζ was found to be EGFR (Figure 1). Our data indicate that EGFR, the transferrin receptor (TfR), and ntcp internalize with similar kinetics (Figure 5) consistent with our previous findings that all

three of these proteins colocalize in early endocytic vesicles (18). These studies show that inhibition of PKCζ activity markedly reduces their internalization (Figure 5). Although PKCζ has been shown to be a downstream target of EGFR (29), a relationship to EGFR internalization has not been demonstrated previously. Further studies with EGFR and ntcp showed that these internalization events are preceded by formation of ruffle-like structures containing these proteins (Figure 7) and that these ruffles are absorbed into the cell following which small extensions containing ntcp and EGFR form, likely representing internalization. Interestingly, ruffle formation requires PKCζ activity (Figure 7B). The mechanism by which PKCζ regulates ruffle formation and internalization is not known, although similar regulation of receptor internalization by PKCζ has been described for notch and the insulin receptor (30,31). The redistribution of ntcp into ruffle structures is maximal with EGF addition as compared to addition of insulin and PDGF, indicating that it is not due to a generalized effect of receptor tyrosine kinase activity (Figure 7D).

That EGFR is an important determinant of ntcp trafficking has been shown in the present experiments. In ntcp-sfGFP expressing HuH7 cells, knockdown of EGFR resulted in a 40% reduction in cell surface expression of ntcp (Figure 4) while total expression remained unchanged (Figure 2). Motility of ntcp-containing endocytic vesicles prepared from EGFR knockdown cells was reduced by about half as compared to vesicles from control cells and was insensitive to inhibition of PKCζ, in contrast to results for control vesicles (Figure 3B). Because of the possibility that lentivirus infection could influence these results, additional studies were performed in endocytic vesicles prepared from cells that had not been exposed to lentivirus. These studies took advantage of the presence of two populations of ntcp-containing endocytic vesicles: one that colocalizes with EGFR and the other that does not. Vesicles associated with both EGFR and ntcp were 3-to 4-fold more motile as compared to vesicles lacking EGFR (Figure 3D). The finding that cell surface, but not total, ntcp is reduced in cells in which EGFR is knocked down (Figure 4) is consistent with its intracellular sequestration in vesicles that are not co-associated with EGFR and have reduced microtubule-based motility and consequently decreased ability to reach the cell surface.

Our studies show that in the absence of EGF, cell surface EGFR and ntcp are in a steady state in which approximately 50% of each protein is on the cell surface and the remainder is intracellular (Figure 4). Addition of EGF results in internalization of EGF-EGFR complexes (Figure 5) and trafficking to lysosomes where the complex is degraded (Figure 6). Ntcp and TfR are also internalized with similar kinetics (Figure 5), but do not undergo degradation, implying that the vesicles containing ntcp/TfR and EGFR are able to segregate these proteins from each other over time. This is consistent with our previous studies *in vitro* showing that endocytic vesicles segregate ntcp and TfR from endocytosed asialoorosomucoid, a ligand that traffics to lysosomes (10,18). In contrast, TfR, which recycles to the plasma membrane following internalization, does not segregate from ntcp in endocytic vesicles (18). Morphologic studies that were now performed using intact HuH7 cells expressing ntcp-sfGFP were in agreement with these findings. As noted above, incubation of these cells with EGF resulted in redistribution of ntcp into ruffle-like structures (Figure 7A). These EGF stimulated structures have been referred to as “circular

dorsal ruffles" and have been shown to function in endocytic internalization as well as cellular motility. Their formation requires EGFR phosphorylation and phosphatidylinositol 3-kinase activity, and can account for 50% of the internalization of ligand bound EGFR (22,23). Incubation of cells with fluorescent EGF induced formation of ntcp-containing ruffles followed by absorption of the ruffles after 8–15 min, presumably at sites of endocytic internalization (22). During ruffle absorption, ntcp was found to colocalize with Fl-EGF at vesicular punctae and this was followed by segregation of ntcp into smaller cell surface extensions and retention of Fl-EGF in the endocytic or late endocytic punctae. This is consistent with the findings that EGF-EGFR traffics to lysosomes while ntcp shuttles between the cell surface and intracellular compartments. These results are also consistent with our previous findings that endocytic vesicles that are simultaneously associated with multiple proteins such as transferrin, asialoorosomucoid, ntcp, and EGFR can undergo fission to efficiently segregate proteins into daughter vesicles with differing subcellular destinations (18). High rates of fission were only seen in early endocytic vesicles, with little seen during later stages of endosome processing (16,17,32,33). We have found that early endocytic vesicles can be associated simultaneously with both minus- and plus-end microtubule-based motors and that a "tug-of-war" process can stretch vesicles, eventually resulting in their fission (34).

Expression of ntcp in transfected cells confers Na^+ dependent bile acid transport with kinetics similar to that in intact liver (1,19). However, the physiological consequences of EGFR regulating ntcp subcellular distribution are not clear. Despite a 40% reduction of cell surface ntcp with EGFR knockdown, there was no effect on uptake kinetics of ^{3}H-taurocholic acid, a known substrate for ntcp (19). It is possible that ntcp exists at the cell surface in two forms, only one of which is competent to transport bile acids. This remains speculative at this time although such a model has been found for several membrane proteins that undergo endocytosis, including the asialoglycoprotein receptor (35,36). Recent studies indicate that human NTCP serves as the receptor for the Hepatitis B virus (2,3,6,37–39) and this very likely involves internalization and trafficking of virus and NTCP through the cell, although this has not yet been examined. Although rodent Ntcp does not mediate Hepatitis B infection in human cells, it may be involved in binding, internalization and trafficking of other ligands or related viruses (3). We suggest that ntcp may have a multifunctional role in hepatocytes, at least one of which is dependent on its subcellular trafficking. This will need to be elucidated in future studies.

Materials and Methods

Chemicals and Reagents

PKCζ pseudosubstrate inhibitor (Cat. No. 539610) was obtained from Calbiochem (San Diego, CA). PNGase F (Cat. No. P0704) was from New England BioLabs (Ipswich, MA). Con A-agarose and WGA-agarose were obtained from Vector laboratories (Burlingame, CA). Protein A HP SpinTrap (Cat. No. 28-9031-32) was from GE Healthcare Life Sciences (Piscataway, NJ). [γ-^{32}P] ATP (Cat. No. NEG502Z) and ^{3}H-taurocholic acid (Cat. No. NET3222) were from PerkinElmer (Waltham, MA). EZ-Link Sulfo-NHS-SS-Biotin (Cat. No. 21328), streptavidin-agarose gel (Cat. No. 20349) and phosphatase inhibitor cocktail

(Cat. No. 78420) were from Thermo Scientific (Rockford, IL). Human EGFR shRNA cloned in lentiviral vector pLKO.1 (Hs_TRC library oligo ID: TRCN0000121068) was purchased from the shRNA Core Facility of the Albert Einstein College of Medicine (Bronx, NY). Mouse monoclonal antibody against EGFR (Cat. No. sc-374607) and rabbit antibody against PKCζ (Cat. No. sc-216) were from Santa Cruz Biotechnology (Santa Cruz, CA). Rabbit antibody against GFP (Cat. No. ab290) was obtained from Abcam (Cambridge, MA). Goat antibody against mouse IgG (H+L) conjugated with HiLyteplus-750 (Cat. No. 61057-05-H750) was from AnaSpec (Fremont, CA). Rabbit antibody to rat ntcp was prepared as previously described (10). All other reagents were from Sigma-Aldrich, St Louis, MO, unless otherwise noted. All chemicals were of analytical grade or higher.

Cell Lines

The human hepatoma cell line HuH7 was obtained from the Animal Models, Stem Cells and Cell Therapy Core of the Marion Bessin Liver Research Center at Einstein. The superfolder GFP plasmid (sfGFP) (40) was provided by the Imaging and Cell Structure Core of the Marion Bessin Liver Research Center at Einstein. cDNA encoding rat ntcp was inserted into the HindIII (5') and BamHI (3') restriction sites of this plasmid after PCR amplification from a pMEP4-ntcp expression plasmid (19), with 5' - CCC AAG CTT CAG AGG ATG GAG GTG CAC AAC GTA TCA GCC CCT – 3' used as sense primer and 5' - GG CGG ATC CGA ATT TGC CAT CTG ACC AGA ATT – 3' used as anti-sense primer. This resulted in expression of ntcp linked to sfGFP at the ntcp C-terminus. All sequences were confirmed by the Sequencing Facility at Einstein. HuH7 cells were transfected with the ntcp-sfGFP plasmid using PolyFect Transfection Reagent (Qiagen, Valencia, CA) according to the manufacturer's protocol and selected for plasmid expression in 200 μg/ml neomycin. Sublines were prepared in which EGFR was knocked down by lentivirus encoding EGFR shRNA or controls in which lentivirus alone was used. shRNA with sense sequence 5′-GCCACAAAGCAGTGAATTTAT-3′, was cloned into lentiviral vector pLKO.1. 293 FTPF cells were cotransfected with this pLKO.1 shRNA vector and with the lentiviral packing vectors pCMV08.91 and VSV.G. The culture supernatant was collected and filtered 24 to 48 h post transfection and was used to infect HuH7-ntcp-sfGFP cells in 60 mm culture dishes by adding 2 ml of lentiviral supernatant and polybrene to a final concentration of 8 μg/ml. At 20 h, the medium was replaced with 5 ml complete RPMI. At 3 days post infection, cells were transferred to 100 mm culture dishes and maintained in RPMI containing G418 (200 μg/ml) and puromycin (2 μg/ml) for selection. Clones were screened for EGFR expression by Western Blot.

Endocytic Vesicle Preparation

Endocytic vesicles were prepared from livers of 200–250 g male Sprague–Dawley rats (Taconic Farms, Germantown, NY) as described previously (16,32,41). Briefly, livers were removed, washed and Dounce homogenized. A postnuclear supernatant was prepared and subjected to Sephacryl S200 (Pharmacia, Uppsala, Sweden) column chromatography. Vesicle enriched fractions were pooled, adjusted to 1.4 M sucrose, and layered at the bottom of a 1.4–1.2–0.25 M discontinuous sucrose density gradient. Following centrifugation at 100,000 g for 2 hours, vesicles were harvested from the 1.2–0.25 M sucrose interface and stored in small aliquots at −80°C until used. All animal procedures were approved by the

Animal Use and Care Committee of the Albert Einstein College of Medicine and appropriate measures were taken to reduce the pain or discomfort of experimental animals. Endocytic vesicles were also prepared from HuH7 cells following a similar procedure as described previously (21,42).

Protein Phosphorylation Assay

Assays were performed on total vesicles or on vesicles that had been immunopurified on protein A-agarose beads to which ntcp antibody was bound. 50 μl of vesicles were incubated at 4°C in 150 μl of MEPS buffer (5 mM $MgSO_4$, 5mM EGTA, 35 mM PIPES-K_2, 0.25 M sucrose) containing protease inhibitor, with and without 75 μM PKCζ inhibitor. After 10 min of incubation, γ-^{32}P-ATP was added to a final concentration of 50 μM (5 μCi) and incubation was continued for 10 min at 4°C. Vesicles were centrifuged, washed, and subjected to SDS-PAGE and radioautography. Whether the phosphoprotein was a glycoprotein was examined by gel shift following incubation with PNGase F according to the manufacturer's instructions. Additional studies were performed to examine binding of this protein, following incubation of phosphorylated vesicles in 1% NP-40, to con A-agarose and WGA-agarose according to the manufacturer's instructions. Studies were also performed to identify proteins eluted from SDS-PAGE gels by LC-MS/MS as we have described previously (42,43).

Immunofluorescence Analysis and Microtubule-based Motility of Vesicles

Vesicles attached to the surface of 5 μl capacity glass microscopy chambers were immunostained for selected proteins using specific antibodies as we have described previously (15,16,41,44). For motility experiments, vesicles were attached to Taxol stabilized fluorescent microtubules that had been bound to the surface of DEAE-dextran precoated microscopy chambers. Following labeling with appropriate primary and fluorescent secondary antibodies, chambers were incubated on a microscope stage at 37°C and 50 μM ATP was added to establish vesicle motility. In some studies, 20 μM PKCζ inhibitor was added to the final wash buffer and the buffer containing ATP. Images were acquired with a 60x 1.4 numerical aperture Olympus objective on an Olympus Ix71 inverted microscope containing automated excitation and emission filter wheels and maintained at 37°C as we have described (10,18). Data were collected through a CoolSNAP HQ cooled charge-coupled device (Photometrics, Roper Scientific, Tucson, AZ) camera regulated by MetaMorph (Molecular Devices, Sunnyvale, CA) software. Cell images were acquired with the above system as well as PhotoFluor metal halide excitation (Chroma Technologies, Bellows Falls, VT) with Dapi, Cy2, Cy3, Cy5 fluorescence and bright-field channels and iXon 897 EMCCD cameras (Andor Technologies, Belfast, Ireland). Fluorescent images were analyzed using ImageJ (National Institutes of Health public domain; rsb.info.nih.gov/ij/) and Adobe Photoshop CS2 version 9.0.2 (Adobe Systems, San Jose, CA). Colocalization of fluorescent vesicles was quantified as we have described previously (10,44). For motility studies, time-lapse movies taken at 1 frame per 1.5 sec for 90 sec were analyzed using ImageJ software by scoring the number of vesicles on microtubules and manually counting those that exhibited movement. Vesicles that moved a distance equal to or greater than 2 vesicle diameters over 90 sec after addition of ATP were scored. Vesicles that were not on microtubules or those that flowed away upon addition of ATP were not scored.

Imaging of Huh7 cells stably transfected with ntcp-sfGFP

Cells were grown to approximately 80% confluence, washed 4 times in serum free medium (SFM, 135 mM NaCl, 1.2 mM $MgCl_2$, 0.8 mM $MgSO_4$, 28 mM dextrose, 2.5 mM $CaCl_2$, and 25 mM Hepes, pH 7.4), incubated with SFM plus 1 μM Hoechst 33342, and imaged under multi-fluorescence time-lapse acquisition at 37°C. Reagents were added as indicated at the microscope. 4 μg/ml biotinylated-EGF linked to Alexa Fluor 555 streptavidin (ThermoFisher # E-35350), was added for 2.5 min followed by washing 5 times in SFM. EGF (Sigma # E9644) was added at 100 ng/mL, PDGF (ThermoFisher # PHG0134) was added at 25, 125, 500 ng / mL, insulin (ThermoFisher # 12585-014) was added at 20 and 100 μg/mL,

Assay of Cell Surface EGFR and Ntcp

Ntcp-sfGFP cells were grown in 60 mm culture plates to 80% confluence. Following washing with ice cold PBS, cells were incubated for 30 min at 4°C in 2 ml PBS containing 0.4 mM EZ-Link Sulfo-NHS-SS-Biotin as per the manufacturer's instructions. Cells were then washed with 50 mM ice cold Tris-HCl, pH 7.5 followed by ice cold PBS. Cells were harvested, placed at −80°C for 20 min, and lysed in 1% NP-40 in PBS. Following centrifugation at 12,000 rpm for 20 min, supernatants were incubated with streptavidin-agarose beads which, following washing, were subjected to SDS-PAGE and Western blot as we have described previously (45).

Assay of EGF-induced degradation of EGFR

Ntcp-sfGFP cells were grown in 60 mm culture plates to 80% confluence and washed 3 times with warm PBS. 5 ml of serum free RPMI was added to each plate and incubated at 37°C for one hour. Recombinant human EGF was added to a final concentration of 100 ng/ml and incubated for 0, 10 or 60 min at 37°C in the presence or absence of PKCζ pseudosubstrate inhibitor. At the end of incubation, culture dishes were cooled on ice, washed 3 times with cold PBS, and harvested. Lysates were prepared in 1% NP-40 and 30 μg of protein was analyzed by Western Blot for EGFR, ntcp, and β-actin.

Assay of internalization of EGFR and ntcp following incubation with EGF

A biotinylation strategy to quantify internalization was used as has been described previously (45–47). In brief, HuH7 cells (2×10^6) stably expressing ntcp-sfGFP in 60 mm culture plates were biotinylated at 4°C for 30 min with 0.5 mg/ml sulfo-NHS-SS-biotin (Pierce) in PBS containing 0.9 mM $CaCl_2$ and 0.33 mM $MgCl_2$ (PBS/CM), pH 7.2. Following washing, they were incubated in ice-cold 50 mM NH_4Cl in PBS/CM for 15 min at 4°C to quench unreacted reagent. Cells were then incubated at 37°C with EGF (100ng/ml) in the presence or absence of 50 μM PKCζ inhibitor for 0, 5 or 10 min to allow internalization of biotin labeled cell surface proteins. Residual biotin on the cell surface was removed by incubation in 50 mM 2-mercaptoethanesulfonic acid (MESNA) in 100 mM Tris·HCl (pH 8.6) containing 100 mM NaCl and 2.5 mM $CaCl_2$ at 4°C for 30 min. Unreacted MESNA was quenched with 5 mg/ml iodoacetamide in PBS/CM at 4°C for 15 min. Biotin-linked protein within the cell was recovered following lysis of cells in 1% NP-40/PBS containing protease inhibitors and incubation for 1 h with 60 μl of a suspension

of streptavidin-agarose beads. Recovered biotinylated internalized protein was analyzed by Western blotting.

Uptake of ^{3}H-Taurocholate by Cells

Uptake of ^{3}H-taurocholic acid was studied as we have described previously over a concentration range of 1–200 μM and normalized to total cell protein (19). Data were fit by non-linear least squares regression (SigmaPlot v. 11.0, Jandel Corporation, San Rafael, CA) to the equation $V=\frac{V_{\max}[S]}{K_m+[S]}+k[S]$ where V represents initial uptake, with [S] denoting the concentration of taurocholate, K_m and V_{max} denoting the Michaelis-Menten constant and the maximum velocity, respectively, and k representing noncarrier-mediated diffusional uptake as we have described previously (19,48). Na^+ dependence of uptake was assayed in some studies in which NaCl in medium was replaced isosmotically by sucrose as we have described previously (49).

Statistical Analysis

Results are expressed as means ± SEM. Statistical analysis was performed using Student's *t*-test or Dunnett analysis after One-way ANOVA as appropriate (Microsoft Excel 2003 and XLSTAT 2014).

Supplementary Material

Refer to Web version on PubMed Central for supplementary material.

Acknowledgements

This work was supported by NIH grants R01 DK23026 and R01 DK098408 to AWW and Liver Pathobiology and Gene Therapy Research Core Center P30 DK041296.

List of Abbreviations

EGFR	epidermal growth factor receptor
ntcp	Na^+-taurocholate cotransporting protein
TfR	transferrin receptor
KD	knockdown
Con A	conconavalin A
WGA	wheat germ agglutinin
PNGase F	Peptide -*N*-Glycosidase F
sfGFP	superfolder GFP

References

1. Meier PJ, Stieger B. Bile salt transporters. Annu.Rev.Physiol. 2002; 64:635–661. [PubMed: 11826283]

2. Yan H, Zhong G, Xu G, He W, Jing Z, Gao Z, Huang Y, Qi Y, Peng B, Wang H, Fu L, Song M, Chen P, Gao W, Ren B, et al. Sodium taurocholate cotransporting polypeptide is a functional receptor for human hepatitis B and D virus. Elife. 2012; 1:e00049. [PubMed: 23150796]
3. Yan H, Peng B, He W, Zhong G, Qi Y, Ren B, Gao Z, Jing Z, Song M, Xu G, Sui J, Li W. Molecular determinants of hepatitis B and D virus entry restriction in mouse sodium taurocholate cotransporting polypeptide. J.Virol. 2013; 87:7977–7991. [PubMed: 23678176]
4. Watashi K, Urban S, Li W, Wakita T. NTCP and beyond: opening the door to unveil hepatitis B virus entry. Int.J.Mol.Sci. 2014; 15:2892–2905. [PubMed: 24557582]
5. Li H, Zhuang Q, Wang Y, Zhang T, Zhao J, Zhang Y, Zhang J, Lin Y, Yuan Q, Xia N, Han J. HBV life cycle is restricted in mouse hepatocytes expressing human NTCP. Cell Mol.Immunol. 2014; 11:175–183. [PubMed: 24509445]
6. Yan H, Peng B, Liu Y, Xu G, He W, Ren B, Jing Z, Sui J, Li W. Viral entry of hepatitis B and d viruses and bile salts transportation share common molecular determinants on sodium taurocholate cotransporting polypeptide. J.Virol. 2014; 88:3273–3284. [PubMed: 24390325]
7. Watashi K, Sluder A, Daito T, Matsunaga S, Ryo A, Nagamori S, Iwamoto M, Nakajima S, Tsukuda S, Borroto-Esoda K, Sugiyama M, Tanaka Y, Kanai Y, Kusuhara H, Mizokami M, et al. Cyclosporin A and its analogs inhibit hepatitis B virus entry into cultured hepatocytes through targeting a membrane transporter, sodium taurocholate cotransporting polypeptide (NTCP). Hepatology. 2014; 59:1726–1737. [PubMed: 24375637]
8. Ni Y, Lempp FA, Mehrle S, Nkongolo S, Kaufman C, Falth M, Stindt J, Koniger C, Nassal M, Kubitz R, Sultmann H, Urban S. Hepatitis B and D Viruses Exploit Sodium Taurocholate Co-transporting Polypeptide for Species-Specific Entry into Hepatocytes. Gastroenterology. 2014; 146:1070–1083. [PubMed: 24361467]
9. Mukhopadhayay S, Ananthanarayanan M, Stieger B, Meier PJ, Suchy FJ, Anwer MS. cAMP increases liver Na+ - taurocholate cotransport by translocating transporter to plasma membranes. Am.J.Physiol. 1997; 273:G842–G848. [PubMed: 9357825]
10. Sarkar S, Bananis E, Nath S, Anwer MS, Wolkoff AW, Murray JW. PKCzeta is required for microtubule-based motility of vesicles containing the ntcp transporter. Traffic. 2006; 7:1078–1091. [PubMed: 16734659]
11. Dranoff JA, McClure M, Burgstahler AD, Denson LA, Crawford AR, Crawford JM, Karpen SJ, Nathanson MH. Short-term regulation of bile acid uptake by microfilament-dependent translocation of rat ntcp to the plasma membrane. Hepatology. 1999; 30:223–229. [PubMed: 10385660]
12. Webster CR, Srinivasulu U, Ananthanarayanan M, Suchy FJ, Anwer MS. Protein kinase B/Akt mediates cAMP- and cell swelling-stimulated Na+/taurocholate cotransport and Ntcp translocation. J.Biol.Chem. 2002; 277:28578–28583. [PubMed: 12034724]
13. McConkey M, Gillin H, Webster CR, Anwer MS. Cross-talk between protein kinases Czeta and B in cyclic AMP-mediated sodium taurocholate co-transporting polypeptide translocation in hepatocytes. J.Biol.Chem. 2004; 279:20882–20888. [PubMed: 15007074]
14. Webster CRL, Anwer MS. Role of the PI3K/PKB signaling pathway in cAMP-mediated translocation of rat liver ntcp. Am.J.Physiol. 1999; 277:G1165–G1172. [PubMed: 10600813]
15. Murray JW, Bananis E, Wolkoff AW. Reconstitution of ATP-dependent movement of endocytic vesicles along microtubules in vitro: an oscillatory bidirectional process. Mol.Biol.Cell. 2000; 11:419–433. [PubMed: 10679004]
16. Bananis E, Murray JW, Stockert RJ, Satir P, Wolkoff AW. Microtubule and motor-dependent endocytic vesicle sorting in vitro. J.Cell Biol. 2000; 151:179–186. [PubMed: 11018063]
17. Bananis E, Nath S, Gordon K, Satir P, Stockert RJ, Murray JW, Wolkoff AW. Microtubule-dependent movement of late endocytic vesicles in vitro: requirements for Dynein and Kinesin. Mol Biol.Cell. 2004; 15:3688–3697. [PubMed: 15181154]
18. Murray JW, Sarkar S, Wolkoff AW. Single vesicle analysis of endocytic fission on microtubules in vitro. Traffic. 2008; 9:833–847. [PubMed: 18284582]
19. Hata S, Wang P, Eftychiou N, Ananthanarayanan M, Batta A, Salen G, Pang KS, Wolkoff AW. Substrate specificities of rat oatp1 and ntcp: implications for hepatic organic anion uptake. Am.J.Physiol Gastrointest.Liver Physiol. 2003; 285:G829–G839. [PubMed: 12842829]

20. Ciechanover A, Schwartz AL, Dautry-Varsat A, Lodish HF. Kinetics of internalization and recycling of transferrin and the transferrin receptor in a human hepatoma cell line. Effect of lysosomotropic agents. J.Biol.Chem. 1983; 258:9681–9689. [PubMed: 6309781]
21. Mukhopadhyay A, Quiroz JA, Wolkoff AW. Rab1a regulates sorting of early endocytic vesicles. Am.J.Physiol Gastrointest.Liver Physiol. 2014; 306:G412–G424. [PubMed: 24407591]
22. Orth JD, Krueger EW, Weller SG, McNiven MA. A novel endocytic mechanism of epidermal growth factor receptor sequestration and internalization. Cancer Res. 2006; 66:3603–3610. [PubMed: 16585185]
23. Hoon JL, Wong WK, Koh CG. Functions and regulation of circular dorsal ruffles. Mol.Cell Biol. 2012; 32:4246–4257. [PubMed: 22927640]
24. Mareninova O, Shin JM, Vagin O, Turdikulova S, Hallen S, Sachs G. Topography of the membrane domain of the liver Na+-dependent bile acid transporter. Biochem. 2005; 44:13702–13712. [PubMed: 16229460]
25. Botham KM, Suckling KE. The effect of dibutyryl cyclic AMP on the uptake of taurocholic acid by isolated rat liver cells. Biochim Biophys Acta. 1986; 883:26–32. [PubMed: 3015232]
26. Grune S, Engelking LR, Anwer MS. Role of intracellular calcium and protein kinases in the activation of hepatic Na+/taurocholate cotransport by cyclic AMP. J.Biol.Chem. 1993; 268:17734–17741. [PubMed: 8394349]
27. Hirai T, Chida K. Protein kinase Czeta (PKCzeta): activation mechanisms and cellular functions. J.Biochem. 2003; 133:1–7. [PubMed: 12761192]
28. Reyland ME. Protein kinase C isoforms: Multi-functional regulators of cell life and death. Front Biosci.(Landmark.Ed). 2009; 14:2386–2399. [PubMed: 19273207]
29. Valkova C, Mertens C, Weisheit S, Imhof D, Liebmann C. Activation by tyrosine phosphorylation as a prerequisite for protein kinase Czeta to mediate epidermal growth factor receptor signaling to ERK. Mol.Cancer Res. 2010; 8:783–797. [PubMed: 20407013]
30. Sjoqvist M, Antfolk D, Ferraris S, Rraklli V, Haga C, Antila C, Mutvei A, Imanishi SY, Holmberg J, Jin S, Eriksson JE, Lendahl U, Sahlgren C. PKCzeta regulates Notch receptor routing and activity in a Notch signaling-dependent manner. Cell Res. 2014; 24:433–450. [PubMed: 24662486]
31. Fiory F, Oriente F, Miele C, Romano C, Trencia A, Alberobello AT, Esposito I, Valentino R, Beguinot F, Formisano P. Protein kinase C-zeta and protein kinase B regulate distinct steps of insulin endocytosis and intracellular sorting. J.Biol.Chem. 2004; 279:11137–11145. [PubMed: 14711831]
32. Bananis E, Murray JW, Stockert RJ, Satir P, Wolkoff AW. Regulation of early endocytic vesicle motility and fission in a reconstituted system. J.Cell Sci. 2003; 116:2749–2761. [PubMed: 12759371]
33. Murray JW, Wolkoff AW. Roles of the cytoskeleton and motor proteins in endocytic sorting. Adv.Drug Deliv.Rev. 2003; 55:1385–1403. [PubMed: 14597137]
34. Nath S, Bananis E, Sarkar S, Stockert RJ, Sperry AO, Murray JW, Wolkoff AW. Kif5B and Kifc1 interact and are required for motility and fission of early endocytic vesicles in mouse liver. Mol Biol Cell. 2007; 18:1839–1849. [PubMed: 17360972]
35. Weigel PH, Oka JA. The dual coated pit pathway hypothesis: vertebrate cells have both ancient and modern coated pit pathways for receptor mediated endocytosis. Biochem.Biophys.Res.Commun. 1998; 246:563–569. [PubMed: 9618251]
36. Shi X, Potvin B, Huang T, Hilgard P, Spray DC, Suadicani SO, Wolkoff AW, Stanley P, Stockert RJ. A novel casein kinase 2a subunit regulates membrane protein traffic in the human hepatoma cell line HuH-7. J.Biol.Chem. 2001; 276:2075–2082. [PubMed: 11038365]
37. Iwamoto M, Watashi K, Tsukuda S, Aly HH, Fukasawa M, Fujimoto A, Suzuki R, Aizaki H, Ito T, Koiwai O, Kusuhara H, Wakita T. Evaluation and identification of hepatitis B virus entry inhibitors using HepG2 cells overexpressing a membrane transporter NTCP. Biochem.Biophys.Res.Commun. 2014; 443:808–813. [PubMed: 24342612]
38. Anwer MS, Stieger B. Sodium-dependent bile salt transporters of the SLC10A transporter family: more than solute transporters. Pflugers Arch. 2014; 466:77–89. [PubMed: 24196564]

39. Oehler N, Volz T, Bhadra OD, Kah J, Allweiss L, Giersch K, Bierwolf J, Riecken K, Pollok JM, Lohse AW, Fehse B, Petersen J, Urban S, Lutgehetmann M, Heeren J, et al. Binding of hepatitis B virus to its cellular receptor alters the expression profile of genes of bile acid metabolism. Hepatology. 2014; 60:1483–1493. [PubMed: 24711282]
40. Pedelacq JD, Cabantous S, Tran T, Terwilliger TC, Waldo GS. Engineering and characterization of a superfolder green fluorescent protein. Nat.Biotechnol. 2006; 24:79–88. [PubMed: 16369541]
41. Murray JW, Wolkoff AW. Assay of Rab4-dependent trafficking on microtubules. Methods Enzymol. 2005; 403:92–107. [PubMed: 16473580]
42. Mukhopadhyay A, Nieves E, Che FY, Wang J, Jin L, Murray JW, Gordon K, Angeletti RH, Wolkoff AW. Proteomic analysis of endocytic vesicles: Rab1a regulates motility of early endocytic vesicles. J.Cell Sci. 2011; 124:765–775. [PubMed: 21303926]
43. Wang P, Wang JJ, Xiao Y, Murray JW, Novikoff PM, Angeletti RH, Orr GA, Lan D, Silver DL, Wolkoff AW. Interaction with PDZK1 is required for expression of organic anion transporting protein 1A1 (OATP1A1) on the hepatocyte surface. J.Biol.Chem. 2005; 280:30143–30149. [PubMed: 15994332]
44. Murray JW, Bananis E, Wolkoff AW. Immunofluorescence microchamber technique for characterizing isolated organelles. Anal.Biochem. 2002
45. Choi JH, Murray JW, Wolkoff AW. PDZK1 binding and serine phosphorylation regulate subcellular trafficking of organic anion transport protein 1a1. Am.J.Physiol Gastrointest Liver Physiol. 2011; 300:G384–G393. [PubMed: 21183661]
46. Nishimura N, Sasaki T. Cell-surface biotinylation to study endocytosis and recycling of occludin. Methods Mol Biol. 2008; 440:89–96. [PubMed: 18369939]
47. Morimoto S, Nishimura N, Terai T, Manabe S, Yamamoto Y, Shinahara W, Miyake H, Tashiro S, Shimada M, Sasaki T. Rab13 mediates the continuous endocytic recycling of occludin to the cell surface. J Biol Chem. 2005; 280:2220–2228. [PubMed: 15528189]
48. Glavy JS, Wu SM, Wang PJ, Orr GA, Wolkoff AW. Down-regulation by extracellular ATP of rat hepatocyte organic anion transport is mediated by serine phosphorylation of oatp1. J.Biol.Chem. 2000; 275:1479–1484. [PubMed: 10625701]
49. Wolkoff AW, Samuelson AC, Johansen KL, Nakata R, Withers DM, Sosiak A. Influence of Cl- on organic anion transport in short-term cultured rat hepatocytes and isolated perfused rat liver. J.Clin.Invest. 1987; 79:1259–1268. [PubMed: 3031134]

Synopsis

Na^+-taurocholate cotransporting polypeptide (ntcp) mediates bile acid transport, also serving as the hepatitis B virus receptor. It traffics in vesicles along microtubules, requiring activity of PKCζ for motility. We have now found that the EGF receptor (EGFR) is the target of PKCζ activity and that EGFR and ntcp colocalize in vesicles. Ntcp-containing vesicles that are not associated with EGFR have reduced microtubule-based motility, consistent with intracellular accumulation and reduced surface expression of ntcp in cells following EGFR knockdown.

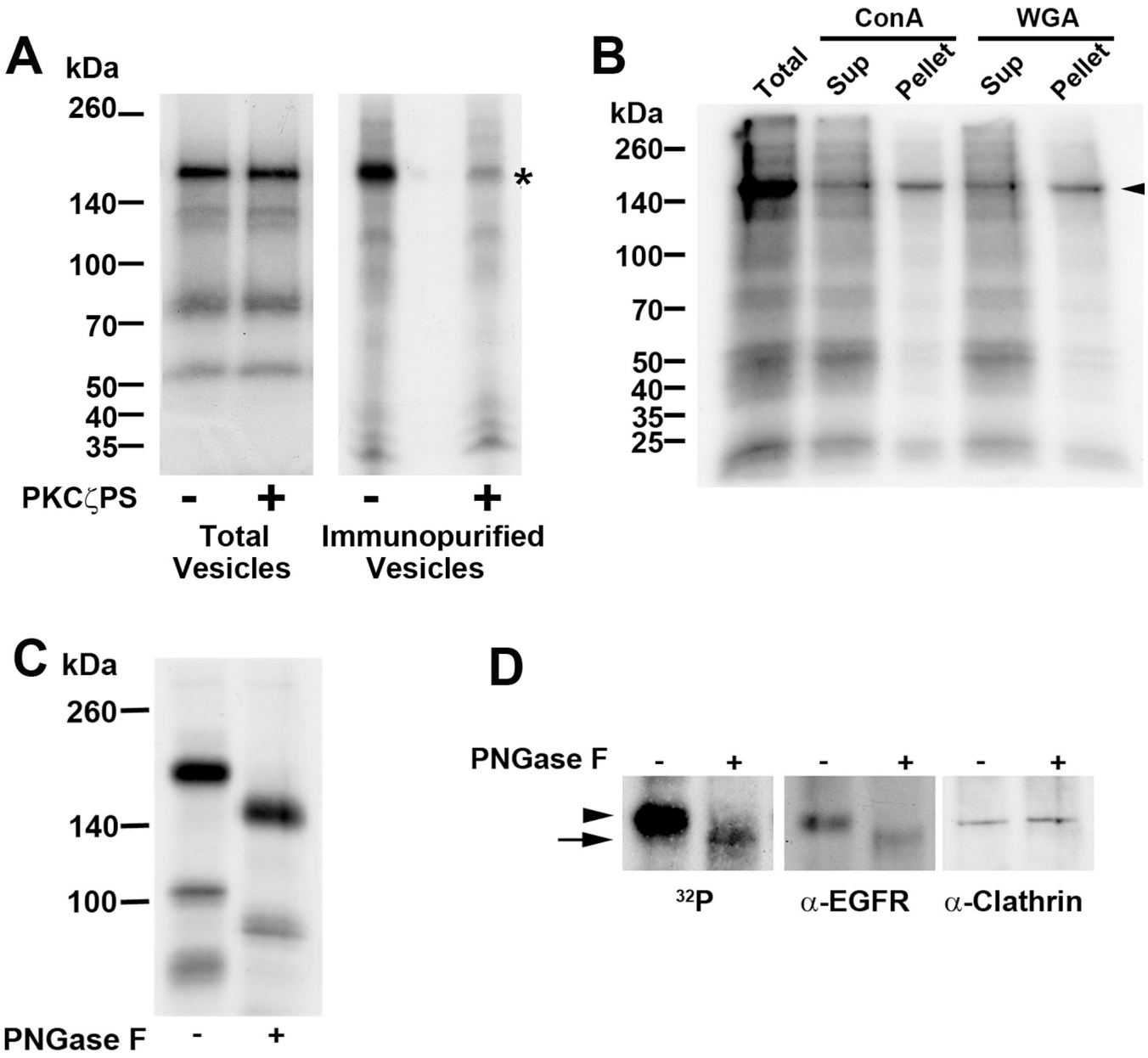

FIGURE 1. Identification of a protein target of PKCζ-mediated phosphorylation in ntcp-containing endocytic vesicles

A. Rat liver derived endocytic vesicles (Total Vesicles) were incubated with γ-^{32}P-ATP in the presence or absence of the PKCζ pseudosubstrate inhibitor (PKCζPS) as indicated. Following SDS-PAGE and radioautography, although several phosphorylated bands were observed when total endocytic vesicles were assayed, none of these bands was sensitive to the protein kinase inhibitor. In contrast, as indicated by the asterisk on the right, when vesicles were first immunopurified using antibody to ntcp linked to agarose beads, a major 180 kDa phosphorylated protein that was sensitive to PKCζ inhibition was seen. B. The protein target of PKCζ in immunopurified ntcp-containing vesicles is a glycoprotein. Immunopurified vesicles were incubated with γ-^{32}P-ATP, solubilized in 1% NP40, and incubated with Con A-agarose or WGA-agarose beads as indicated. After centrifugation,

supernatant and beads (pellet) were subjected to SDS-PAGE and radioautography. The 180 kDa protein was recovered in both pellets, as indicated by the arrowhead. C. The protein target of PKCζ in immunopurified ntcp-containing vesicles is an N-linked glycoprotein. Immunopurified vesicles were incubated with γ-^{32}P-ATP before incubation without and with PNGase F. This resulted in a mobility shift from 180 kDa to 140 kDa following SDS-PAGE and radioautography, consistent with removal of N-linked carbohydrate. D. The protein target of PKCζ in immunopurified ntcp-containing vesicles migrates with EGFR on SDS-PAGE. Mass spectroscopy indicated that the 180 kDa band contained EGFR and clathrin. In this study, following incubation with γ-^{32}P-ATP, ntcp immunopurified vesicles were subjected to SDS-PAGE and radioautography or Western blot for EGFR and clathrin. Radioactivity and both proteins migrated at 180 kDa as indicated by the arrowhead. Following incubation with PNGase F, radioactivity and EGFR migrated faster and coincided, as indicated by the arrow. Migration of clathrin was unchanged. All panels in this figure show representative studies of 3 or more experiments.

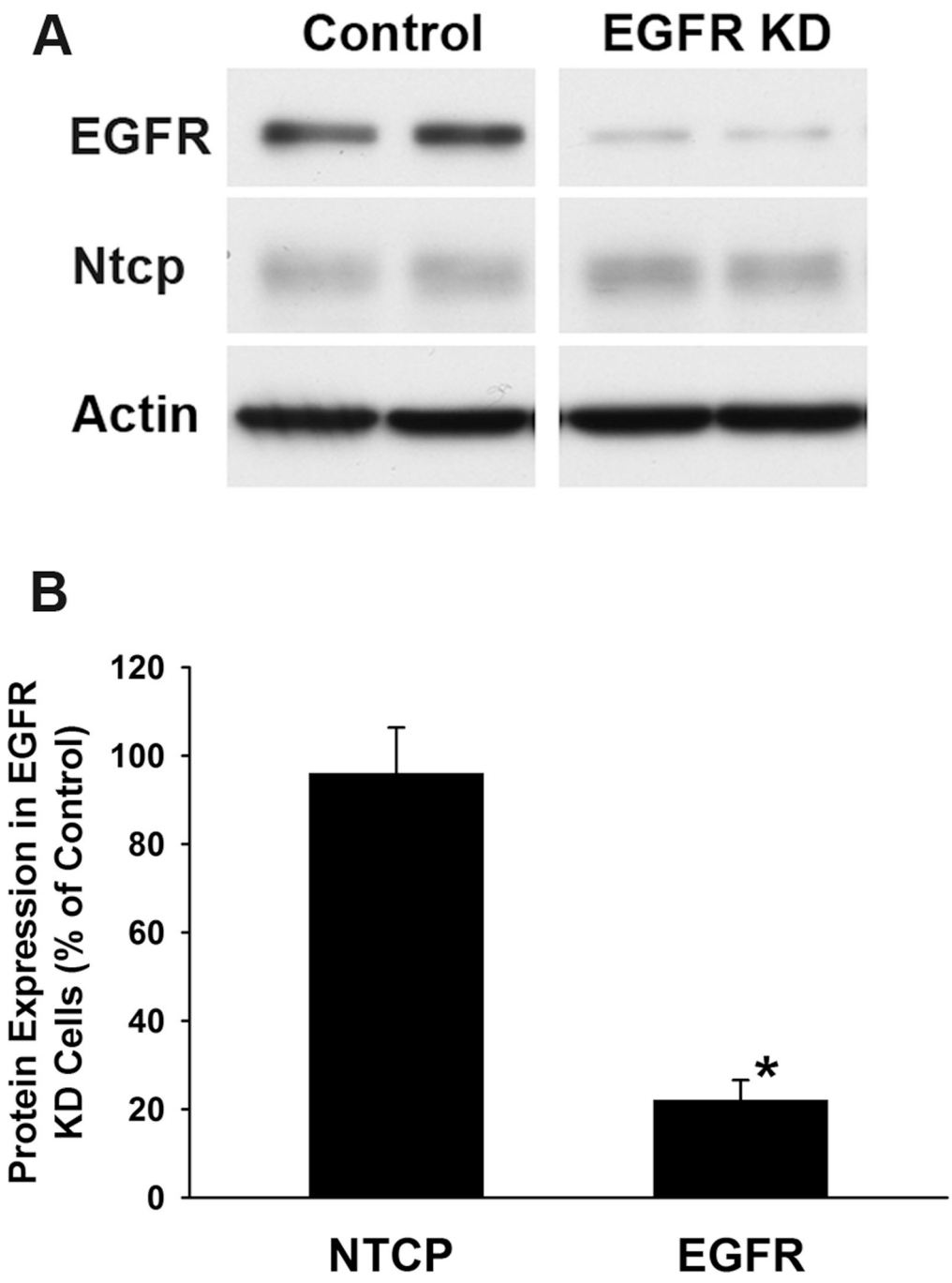

FIGURE 2. Knockdown of EGFR does not affect ntcp expression

EGFR knockdown was performed by infection of HuH7 cells expressing ntcp-sfGFP with lentivirus encoding shRNA to EGFR as described in Methods. Control cells were infected with lentivirus containing empty vector. Expression of EGFR and ntcp was determined in total cell lysates by Western blot. A. Representative study in which a single gel was run, transferred to nitrocellulose, and divided horizontally to probe with each antibody. The vertical divide between control and EGFR lanes was done to put the different sections of a single gel together for the figure. Each lysate was run in duplicate lanes. B. Four

independent studies were performed as in panel A, and Western blots were quantified by densitometry and normalized for actin expression. The bars represent expression of ntcp or EGFR, as indicated, in EGFR knockdown cells as compared to control cells that were infected with lentivirus containing empty vector. Results are expressed as mean ± SEM. *$p<0.01$.

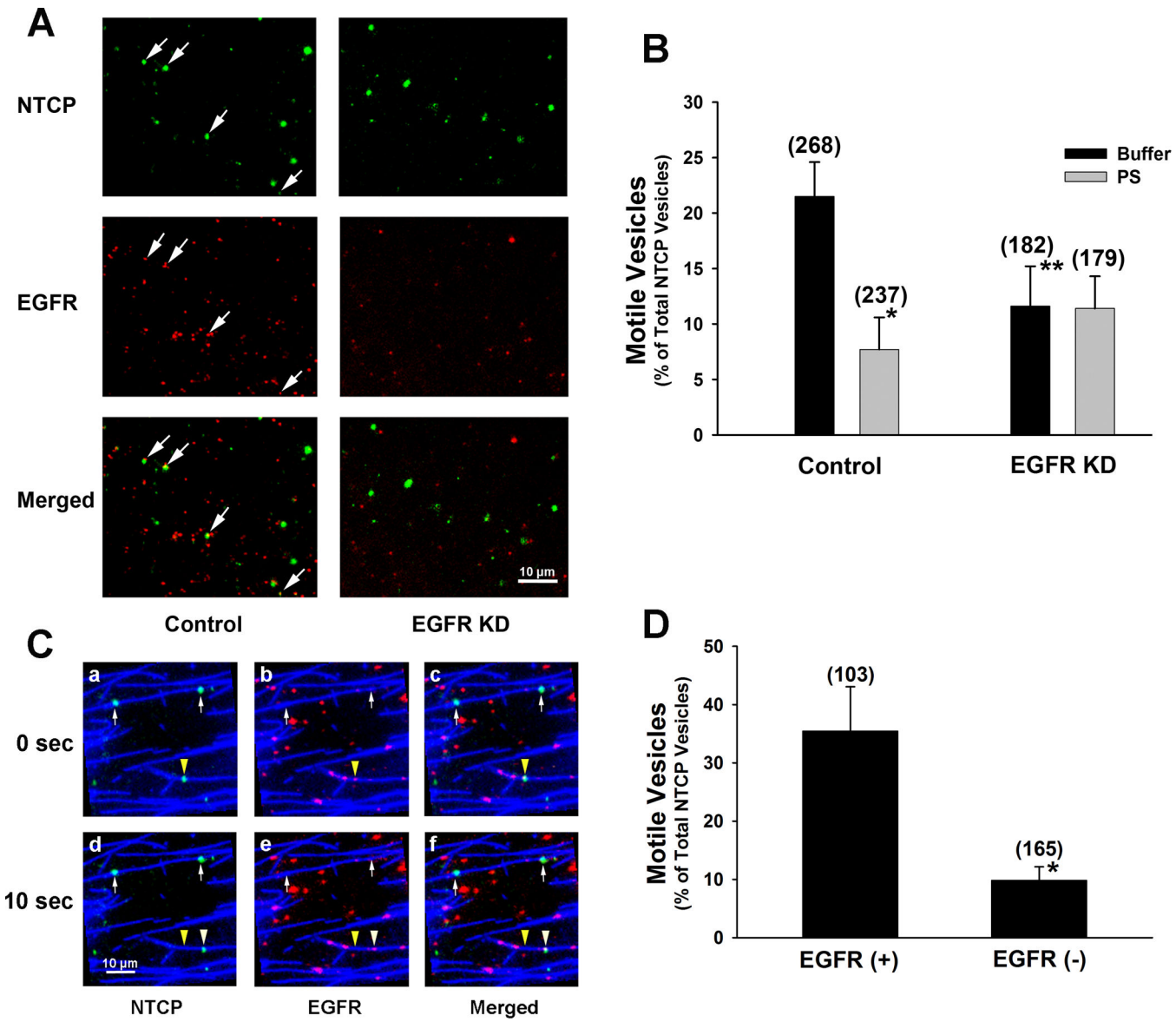

FIGURE 3. Effect of colocalization with EGFR on motility of ntcp-containing vesicles on microtubules

A. Localization of EGFR (red) and ntcp (green) in endocytic vesicles prepared from EGFR knockdown (KD) or lentiviral vector alone infected (control) HuH7 cells expressing ntcp-sfGFP. Some vesicles in which EGFR and ntcp are colocalized (merged) are indicated by the arrows. There was little colocalization in the EGFR knockdown vesicles. B. Microtubule-based motility of ntcp-containing endocytic vesicles prepared from EGFR knockdown cells is reduced as compared to vesicles prepared from lentiviral vector alone infected (control) cells and is insensitive to inhibition of PKCζ. The percentage of ntcp containing vesicles, prepared from control and EGFR knockdown cells that move on microtubules in microtubule-coated microscopy chambers is shown. Motility was assayed in the presence of ATP alone (buffer) or in the presence of ATP plus PKCζ pseudosubstrate inhibitor (PS). Numbers of vesicles that were assayed are in parentheses. Results are

expressed as mean ± SEM. *p<0.01 as compared to control. ** p<0.03 as compared to control. C. In the absence of EGFR, ntcp-containing vesicles have reduced motility. Endocytic vesicles prepared from HuH7 cells expressing ntcp-sfGFP (green) that had not been infected with lentivirus were attached to fluorescent microtubules (blue) in a microscopy chamber and immunostained with antibody to EGFR (red). Panels, as indicated, are shown at 0 and 10 sec after addition of 50 μM ATP for ntcp (green, panels a and d) and EGFR (red, panels b and e) as well as merged views (panels c and f). The arrowhead indicates the position of a vesicle that contains both ntcp and EGFR. The yellow arrowhead marks the initial position, and the white arrowhead marks the position of this vesicle after movement. The arrows indicate vesicles that contain ntcp but not EGFR. These vesicles did not move. D. Ntcp-containing vesicles that colocalize with EGFR have increased microtubule-based motility as compared to those that do not colocalize with EGFR. Experiments were performed in HuH7 cells expressing ntcp-sfGFP that had not been infected with lentivirus. The numbers of vesicles that were assayed is in parentheses. Results are expressed as mean ± SEM. *p<0.01.

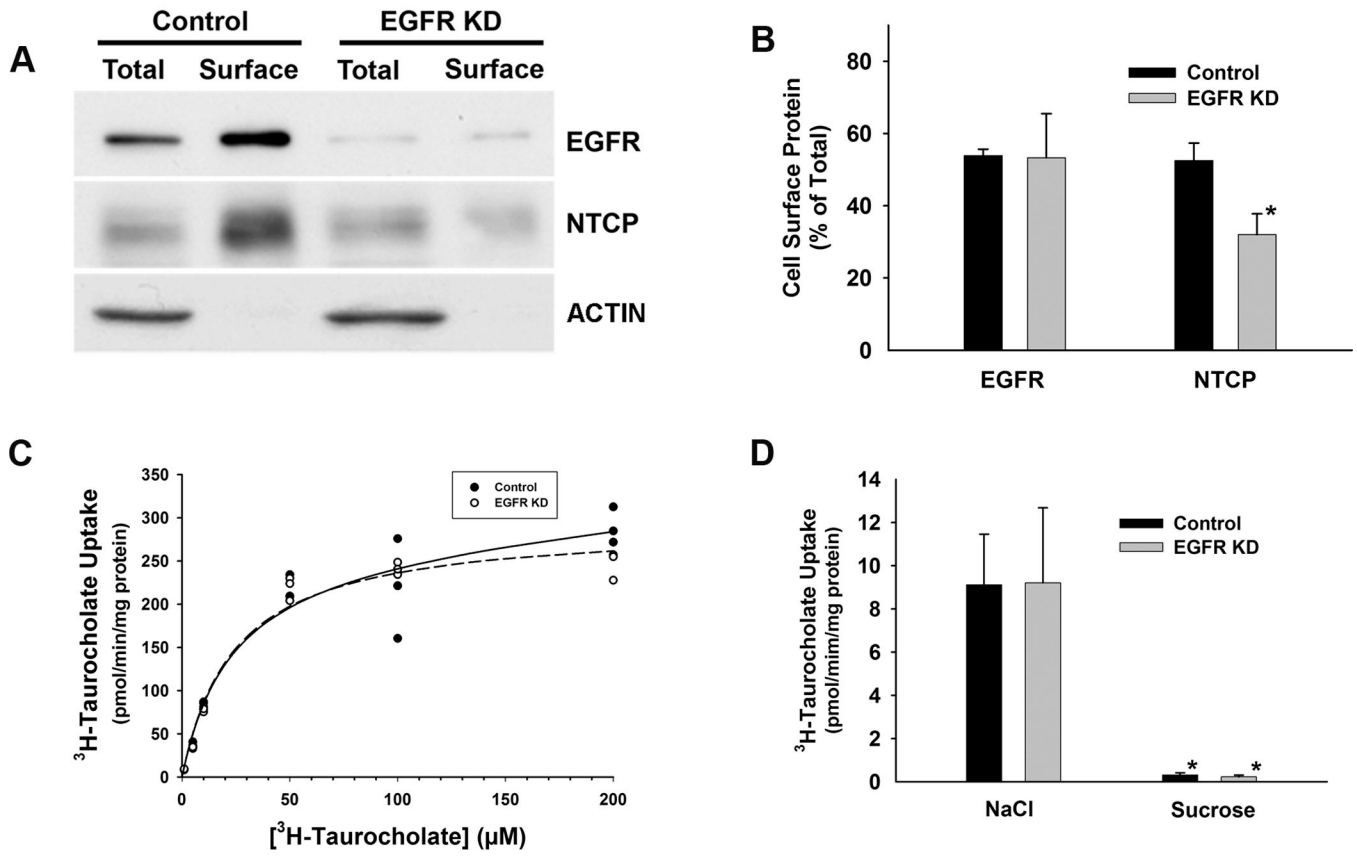

FIGURE 4. EGFR knockdown results in reduced cell surface expression of ntcp but has no effect on kinetics of ^{3}H-taurocholate transport

A. Biotinylation assay to quantify cell surface EGFR and ntcp in control and EGFR knockdown (KD) cells. Cells were biotinylated with a cell impermeable reagent as described in Methods. Cell lysates were prepared and biotinylated proteins were captured on streptavidin-agarose beads and analyzed by Western blot for content of EGFR, ntcp, and actin. Results were compared with an aliquot of lysate ("Total") to permit quantification of total protein expression. In this representative study of four that were performed, 15 μg of cell protein was analyzed in each "Total" lane and 34 μg in each "Surface" lane. Biotinylated actin was not detected in the surface pulldown, consistent with its intracellular localization, and serving as a control for the specificity of the biotinylation assay. B. Quantification of cell surface EGFR and ntcp in control and EGFR knockdown cells. Results of four studies are shown. Results are expressed as mean ± SEM. *$p<0.04$ as compared to control. C. Saturation kinetics of uptake of ^{3}H-taurocholic acid by control lentiviral vector only infected cells and EGFR knockdown cells that express ntcp-sfGFP. In this representative study of 3 that were performed, K_m was 22.9 and 24.2 μM for control and EGFR knockdown cells respectively. V_{max} was 271 and 293 pmol/min/mg protein, respectively and k was 0.2 and $3x10^{-8}$ μl/min/mg protein, respectively. The lines represent the computer fit to the experimental data represented by the circles. D. Uptake of ^{3}H-taurocholic acid by control lentiviral vector only infected cells and EGFR knockdown cells that express ntcp-sfGFP is Na^+-dependent. Initial uptake of 1 μM ^{3}H-taurocholic acid was determined in medium containing NaCl and medium in which NaCl was replaced

isosmotically by sucrose as in Methods. Six paired studies were performed, each in triplicate and mean ± SEM are shown. Uptake was reduced by over 95% in the absence of NaCl ($p<0.04$) and there was no difference between uptake by control lentiviral vector only infected cells and EGFR knockdown cells that express ntcp-sfGFP ($p > 0.9$).

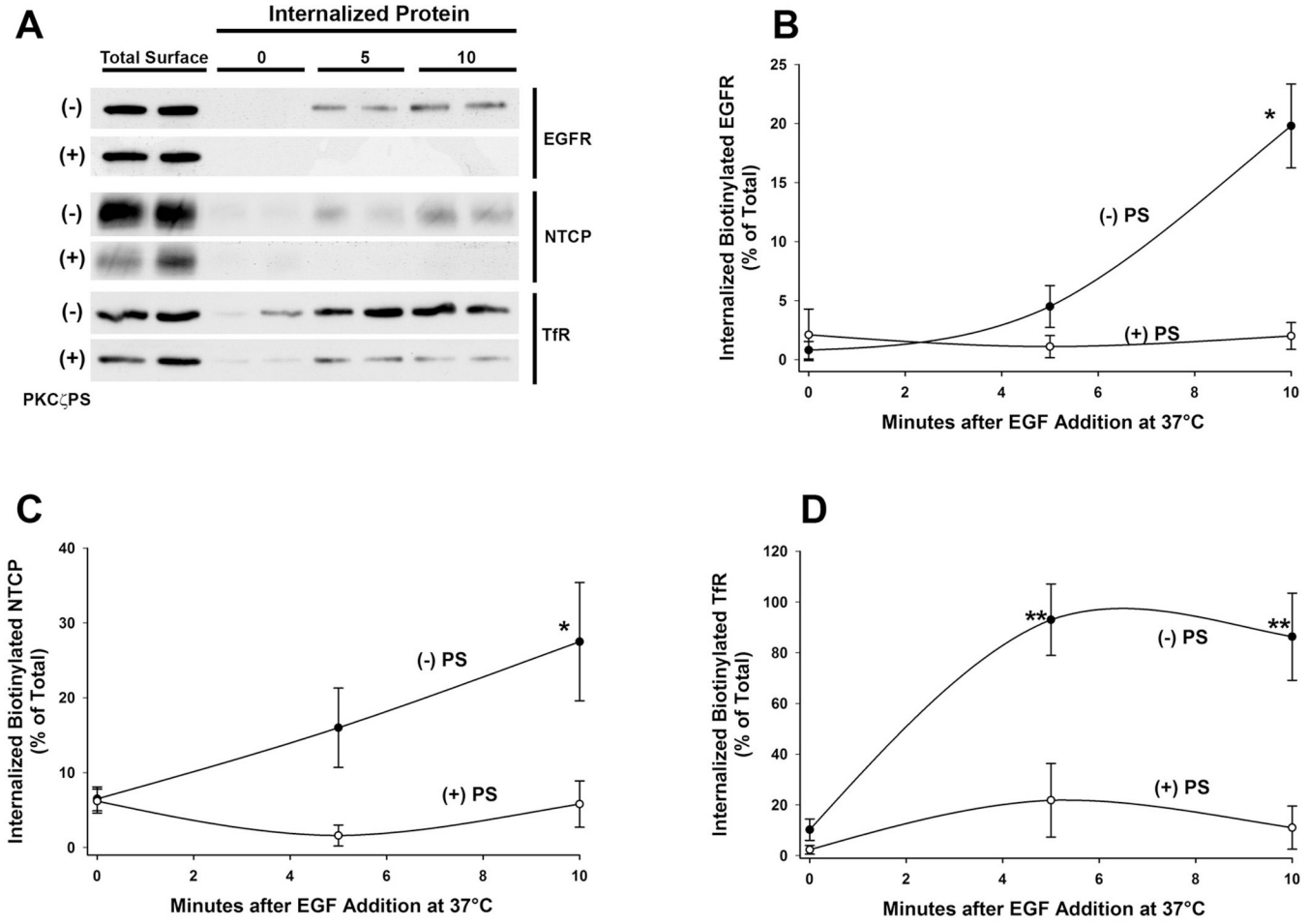

FIGURE 5. Internalization of EGFR and ntcp following incubation with EGF

HuH7 cells stably transfected with ntcp-sfGFP were plated on 60 mm cell culture dishes (2 x 10^6 cells/plate). Cells were surface biotinylated with membrane-impermeant sulfo-NHS-SS-biotin for 30 min at 4°C, followed by EGF addition and incubation at 37°C for 0, 5, or 10 min, in the presence or absence of PKCζ pseudosubstrate inhibitor (PKCζPS), to allow internalization of biotinylated proteins. After removal of residual biotin from the cell surface by reduction, internalized biotinylated surface proteins were collected on streptavidin-agarose beads and subjected to immunoblot for EGFR, ntcp, and TfR. A. Western blot image of a representative experiment with lanes loaded in duplicate. Total Surface represents cells in the absence of biotin reduction. Times are minutes after EGF addition as indicated.. B, C, and D. Results of densitometric quantitation of 3 individual experiments for EGFR, ntcp, and TfR respectively. Data were normalized to total starting cell surface biotinylated EGFR. ntcp, or TfR. Results are expressed as mean ± SEM. *$p<0.03$ and **$p<0.01$ as compared to time zero control.

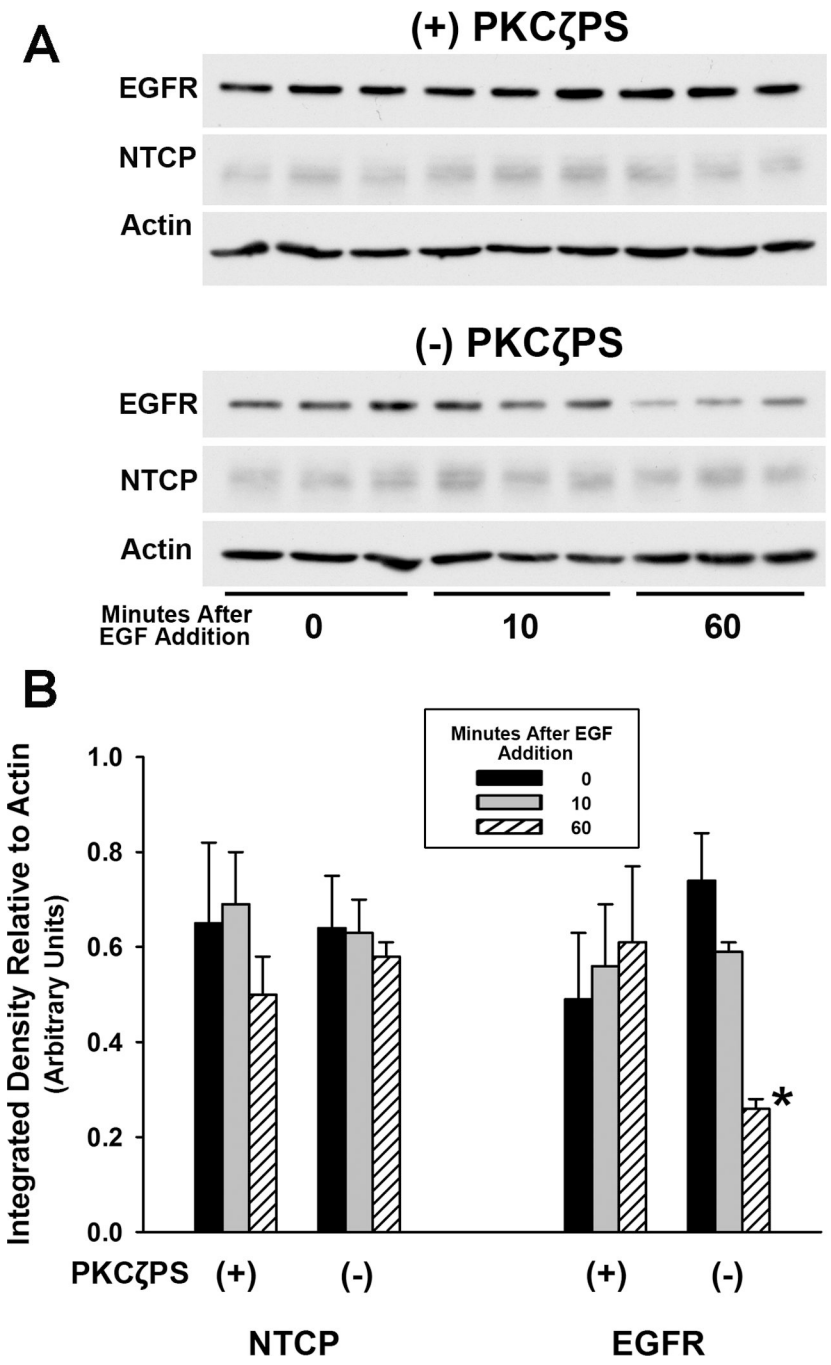

FIGURE 6. Divergence of subcellular trafficking of EGFR and ntcp

A. HuH7 cells expressing ntcp-sfGFP were incubated with EGF with or without PKCζ pseudosubstrate inhibitor (PKCζPS) for up to 60 min. Cell lysates were examined in triplicate in this representative Western blot. There was no change in EGFR content when PKCζ activity was inhibited (top panel). In contrast, without inhibition of PKCζ, EGFR, but not ntcp, trafficked to lysosomes and was degraded, as seen by reduced band intensity on the Western blot (lower panel). B. Densitometric quantitation of three experiments performed as

in panel A. Results were normalized to actin content and are expressed as mean ± SEM..
*p<0.01.

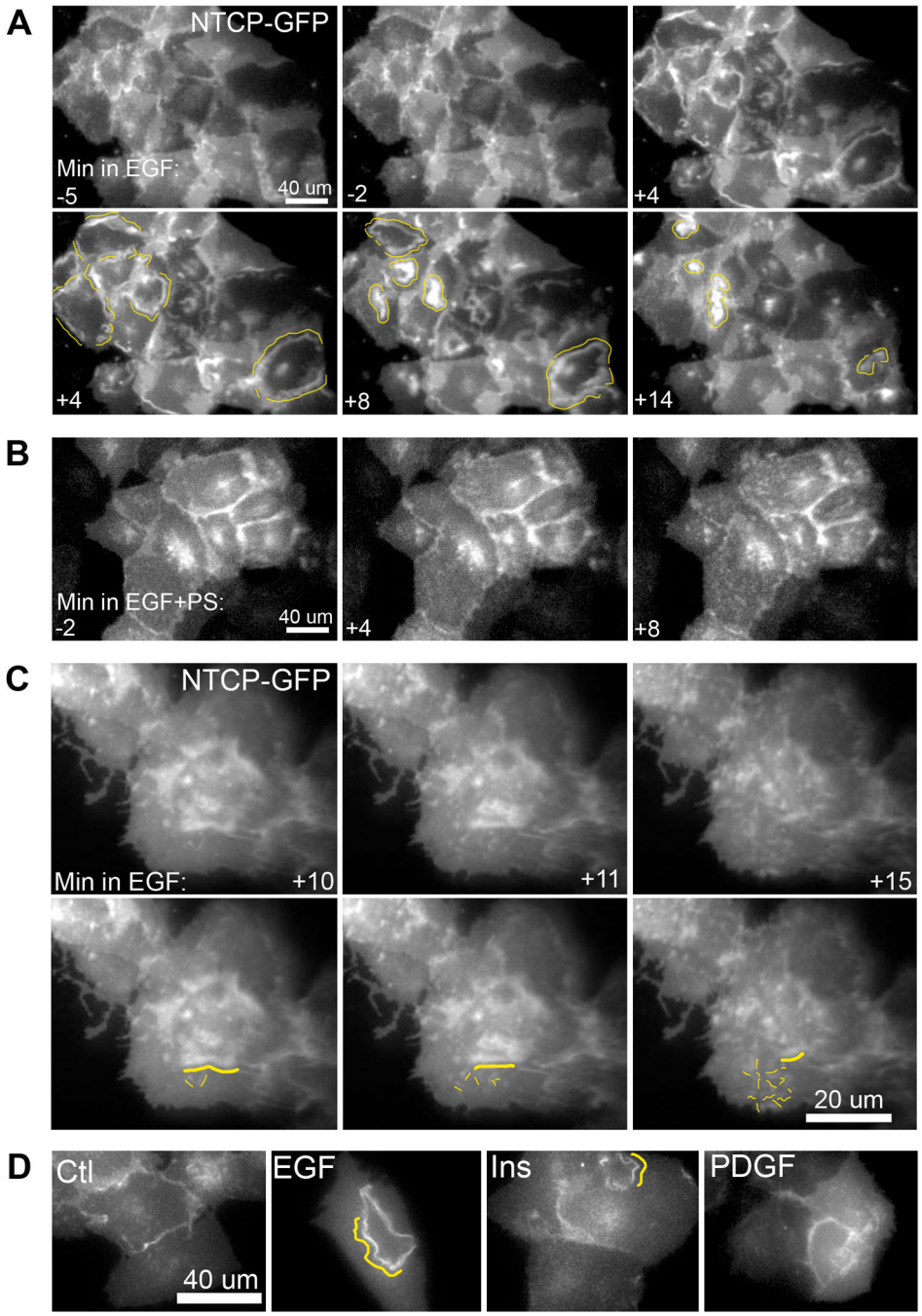

Figure 7. EGF induces ntcp-sfGFP containing ruffling that is blocked by inhibition of PKCζ

Ntcp-sfGFP expressing Huh7 cells were cultured on glass-bottomed chambers and imaged under live cell fluorescence microscopy. A. At time 0, EGF (100 ng/ml) was added to the chamber and cells were imaged in the ntcp-sfGFP channel for an additional 15 min at 1 frame per min. At time points prior to EGF addition ruffles are not seen. Yellow lines indicate ntcp-sfGFP containing ruffles that form and move centripetally across cells before being absorbed (supplementary movie 1). B. In the presence of 12.5 μM PKCζ pseudosubstrate inhibitor (EGF+PS), ruffle formation is inhibited. Time in minutes is at the

lower left of each panel (supplementary movie 2). C. Higher magnification imaging reveals that as ruffles are absorbed into the cell, small extensions containing ntcp form throughout the cell. Duplicate images with lines drawn highlight a ruffle reabsorbing into the cell (yellow line) and new extensions (smaller yellow lines; supplementary movie 3). D. Representative images demonstrate Ntcp-sfGFP-containing ruffle induction for ligands of three receptor tyrosine kinases, Ctl (buffer alone), EGF (100 ng/mL), insulin (20 ug/mL), PDGF (500 ng / mL). EGF induced substantial ntcp containing ruffles while insulin induced some ruffles, but PDGF and buffer alone did not alter ntcp distribution.

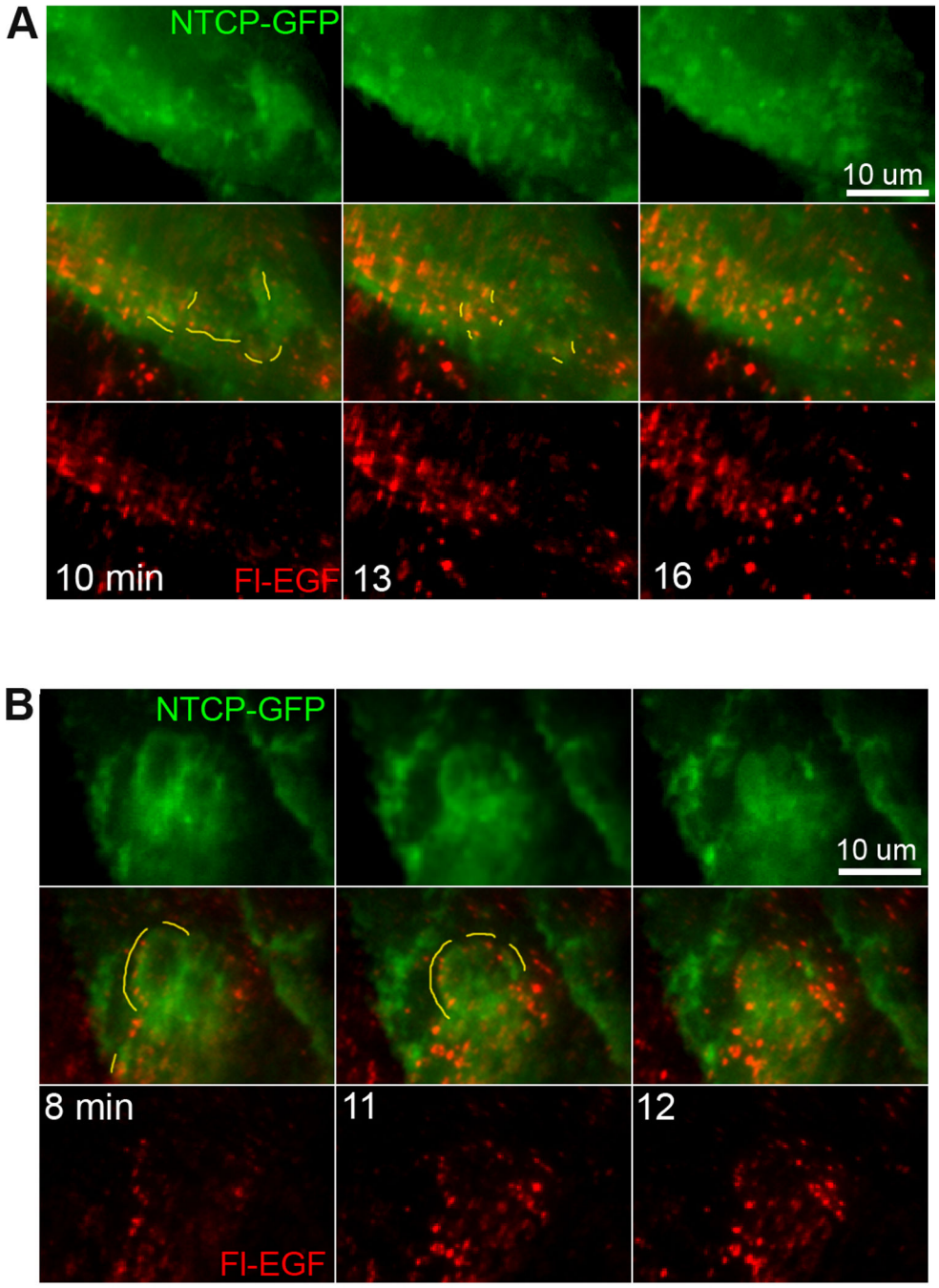

Figure 8. Reabsorption of ntcp-containing ruffles occurs at sites of colocalization between ntcp and fluorescent EGF

High magnification live imaging was performed as in Figure 7C after the addition of fluorescent EGF (red) to HuH7 cells expressing ntcp-sfGFP (green; supplementary movies 4, 5). Ruffles were induced and were subsequently reabsorbed into the cells as highlighted by yellow lines. These reabsorption sites also contained coalescing fluorescent EGF that had been endocytosed by the cells. A and B provide two examples of this phenomenon. Some cells did not show visible expression of ntcp-sfGFP. Time in minutes is indicated.

Table 1

Non-linear Regression Fit of ^{3}H-Taurocholate Uptake in Vector Control and EGFR Knockdown Cells

	n	K_m (μM)	V_{max} (pmol/min/mg protein)	k (μl/min/mg protein)
Vector Control	3	16.9 ± 7.5	265.7 ± 28.1	0.31 ± 0.24
EGFR KD	3	19.1 ± 10.9*	294.0 ± 41.4*	0.46 ± 0.79*

Uptake of ^{3}H-taurocholate was quantified and analyzed by non-linear regression to the equation $V=\frac{V_{\max}[S]}{K_m+[S]}+k[S]$ where *V* represents initial uptake, with [*S*] denoting the concentration of ^{3}H-Taurocholate, K_m and V_{max} denoting the Michaelis-Menten constant and the maximum velocity, respectively, and *k* representing noncarrier-mediated diffusional uptake. n is the number of studies performed.

* $p > 0.5$ vs control.